Plakophilin 2 Affects Cell Migration by Modulating Focal Adhesion Dynamics and Integrin Protein Expression

Jennifer L. Koetsier[1], **Evangeline V. Amargo**[1], **Viktor Todorovi** [1], **Kathleen J. Green**[1,2], and **Lisa M. Godsel**[1,2]

[1]Department of Pathology, Northwestern University Feinberg School of Medicine, Chicago, Illinois, USA

[2]Department of Dermatology, Northwestern University Feinberg School of Medicine, Chicago, Illinois, USA

Abstract

Plakophilin 2 (PKP2), a desmosome component, modulates the activity and localization of the small GTPase RhoA at sites of cell–cell contact. PKP2 regulates cortical actin rearrangement during junction formation, and its loss is accompanied by an increase in actin stress fibers. We hypothesized that PKP2 may regulate focal adhesion dynamics and cell migration. Here we show that PKP2-deficient cells bind efficiently to the extracellular matrix, but upon spreading display total cell areas ~30% smaller than control cells. Focal adhesions in PKP2-deficient cells are ~2× larger and more stable than in control cells, and vinculin displays an increased time for fluorescence recovery after photobleaching. Furthermore, β4 and β1 integrin protein and mRNA expression is elevated in PKP2-silenced cells. Normal focal adhesion phenotypes can be restored in PKP2-null cells by dampening the RhoA pathway or silencing β1 integrin. However, integrin expression levels are not restored by RhoA signaling inhibition. These data uncover a potential role for PKP2 upstream of β1 integrin and RhoA in integrating cell–cell and cell–substrate contact signaling in basal keratinocytes necessary for the morphogenesis, homeostasis, and reepithelialization of the stratified epidermis.

INTRODUCTION

Plakophilins (PKPs) are members of the p120[ctn] subfamily of armadillo proteins with nine central, fairly well-conserved armadillo repeat domains flanked by less well-conserved amino- and carboxy-terminal domains (Hatzfeld, 2007). PKPs are constituents of the intercellular adhesive junctions, desmosomes, which are organelles important for the integrity of tissues, particularly those that experience mechanical stress such as skin and

CONFLICT OF INTEREST
The authors state no conflict of interest.

SUPPLEMENTARY MATERIAL
Supplementary material is linked to the online version of the paper at http://www.nature.com/jid

heart. Plakophilin family members (PKP 1–3) are expressed in distinct patterns within the layers of stratified epidermis, with PKP2 mainly expressed in the basal cell layer (Hatzfeld, 2007; Bass-Zubek *et al.,* 2009). PKP1 mutations lead to the human disorder ectodermal dysplasia and skin fragility, whereas PKP3 deficiency in mice results in hair follicle abnormalities and dermatitis (Sklyarova *et al.,* 2008; McGrath and Mellerio, 2010). PKP2 is the only PKP found in cardiac tissue, where it is required for the morphogenesis and function of the heart. Mutations in PKP2 are linked to the cardiac disease, arrhythmogenic right ventricular cardiomyopathy, although the mechanisms that cause the arrhythmias are poorly understood (Bolling and Jonkman, 2009; Rickelt and Pieperhoff, 2012). Skin phenotypes have not yet been linked to PKP2 mutations, and as skin examinations of cardiac patients are not routinely performed, it is an open question as to whether the arrhythmogenic right ventricular cardiomyopathy mutations are also linked to skin abnormalities.

PKPs are located at the membrane, in the cytoplasm, and in the nucleus. PKPs act as a structural scaffold for desmosome formation, clustering, and maturation through interactions with the desmosomal cadherins, desmoplakin, intermediate filaments, and perhaps actin (Hatzfeld *et al.,* 2000; Chen *et al.,* 2002; Bonne *et al.,* 2003). In addition, their association with nuclear and regulatory proteins suggests that they can function as signaling modulators important for tissue differentiation, cell–cell contact formation, and migration (Green and Simpson, 2007; Bass-Zubek *et al.,* 2009; Getsios *et al.,* 2009; Godsel *et al.,* 2010; Green *et al.,* 2010; Thomason *et al.,* 2010).

PKPs have potential roles in transcription and translation, as PKP2 is a component of the polymerase III holoenzyme and PKP3 associates with ribonucleoprotein particles containing stalled translation initiation complexes (Mertens *et al.,* 2001; Hofmann *et al.,* 2006). PKP1 has been shown to associate with single-stranded DNA and may be involved in the response to DNA damage. It also interacts with the translation initiation factor eIF4A1 to promote translation (Sobolik-Delmaire *et al.,* 2010; Wolf *et al.,* 2010). Finally, our data support the hypothesis that PKP2 acts as a signaling scaffold that functionally links RhoA– and protein kinase C–dependent pathways to drive actin reorganization and regulate desmosome assembly (Bass-Zubek *et al.,* 2008; Godsel *et al.,* 2010).

Previously, we demonstrated that PKP2 deficiency resulted in an increase in the global cellular activity of the small GTPase, RhoA, coupled with a failure of RhoA to localize to sites of cell–cell contact (Godsel *et al.,* 2010). Concomitantly, we observed an accumulation of actin stress fibers at the expense of the typical cortical actin arrangement exhibited by epithelial cells (Zhang *et al.,* 2005). These changes disrupted the formation and maturation of desmosome junctions. We hypothesized that the global change in RhoA activity may also affect cell–substrate attachments, including integrin-based focal adhesions, as such adhesions are known to regulate cell behavior via functional interactions with small GTPases and the actin cytoskeleton (Hamill *et al.,* 2009; Hamill *et al.,* 2010; Hamill *et al.,* 2011; Tsuruta *et al.,* 2011; Hong *et al.,* 2012). We set out to address the possibility that PKP2 functions to integrate signals within the keratinocyte adhesive network of both cadherin- and integrin-based adhesions.

Here we show that genetic interference with PKP2 alters cell spreading and migration, accompanied by changes in focal adhesion dynamics and composition, including elevation of both β1 and β4 integrin expression. Alterations in RhoA activity and integrin expression are, at least in part, causally related to these cellular changes, as decreasing RhoA activity or β1 integrin silencing in PKP2-null cells reverses focal adhesion phenotypes to those seen in control cells. Collectively, these data support a potential role for PKP2 in integrating cell–cell and cell–substrate contact signaling. PKP2 may function either through a pathway in which integrins are upstream of RhoA or in a scenario in which PKP2 regulates integrins and RhoA in separate processes, both having an impact on cell contacts.

RESULTS AND DISCUSSION

PKP2 is necessary for efficient epithelial cell spreading

Our previous work implicated PKP2 as a signaling scaffold, regulating the localization of RhoA within epithelial cells. In the absence of PKP2, RhoA activity failed to accumulate at sites of nascent cell–cell contact, and its activity markedly increased (Godsel *et al.,* 2010). We surmised that the absence of PKP2 may affect other adhesive structures, such as integrin-based cell–substrate junctions. Thus, we set out to examine the interaction between PKP2-deficient keratinocytes and the underlying substrate during attachment, spreading, and migration, using SCC9s, an oral squamous cell line, and primary normal human epidermal keratinocytes (NHEKs).

Control (CTL) small interfering RNA (siRNA)–treated NHEK cells (CTL knockdown (KD)) or cells silenced for PKP2 (PKP2 KD) were stained to analyze PKP2 expression, and correlated with the presence or absence of siGLO, a marker of siRNA uptake efficiency (Figure 1a). In all, 89% of the NHEKs were silenced for PKP2 expression that correlated with the presence of siGLO, whereas 4% of the PKP2-silenced cells did not exhibit siGLO fluorescence. Of those cells that still retained PKP2 expression, only 5% contained siGLO. Similar results were obtained with the SCC9 cell line (Supplementary Figure S1a online). CTL KD or PKP2 KD cells were plated on predeposited collagen I or collagen IV matrix for 30 minutes, and the adherent population was then measured using crystal violet staining and spectrometry. Cells lacking PKP2 adhered better than the control population to both matrix molecules. In all, 85% of the PKP2 KD cells adhered to collagen I and >60% to collagen IV compared with 70% and 45% of the CTL KD NHEKs binding to collagen I and IV matrix, respectively (Figure 1b). PKP2 KD cells attached to the substrate for 30 minutes exhibited a tight, but circular, morphology (Figure 1c), as did the control cells; similarly, under steady-state conditions, control and PKP2 KD cells were similar in size. However, PKP2 KD cells did not spread out as extensively as the control population, displaying cell areas ~30% smaller than those of the control cell population (Figure 1d). The difference in spreading was observed over time using differential interference contrast live-cell imaging, demonstrating that cell spreading is hindered up to at least 75 minutes after attachment (Figure 1e).

Prominent focal adhesions are observed in PKP2-deficient keratinocytes

We hypothesized that the inefficiency of PKP2 KD cell spreading could be due to the behavior or composition of the focal adhesions formed at the time of attachment (Schober *et al.,* 2007). We first analyzed the expression of focal adhesion components in control and PKP2 KD keratinocytes. Immunoblot analysis determined that both populations expressed the full complement of the focal adhesion proteins such as talin, vinculin, zyxin, and focal adhesion kinase (Figure 2a). Changes in focal adhesion kinase could account for some of the phenotypes described below; therefore, we analyzed the amount of active, phosphorylated focal adhesion kinase, finding that it did not change upon PKP2 KD (Ren *et al.,* 2000). Paxillin and zyxin localized to the focal adhesions of both the control and PKP2 KD cells (Figure 2b). However, PKP2 KD cells contained more mature focal adhesions, as reflected in part by two indicators of stable adhesions, greater zyxin, and lower phospho-paxillin content compared with the adhesions in control cells, as measured by pixel intensities (Yoshigi *et al.,* 2005; Hoffman *et al.,* 2006; Choi *et al.,* 2011) (Figure 2c). In addition, focal adhesion size, another indicator of maturity, was, on average, ~2 times greater in the PKP2 KD cells than in the control population (Choi *et al.,* 2011) (Figure 2d). These larger focal adhesions were associated with larger actin bundles (Figure 2e) (Hall, 1998). The efficient silencing of PKP2 in NHEKs and the corresponding increase in zyxin accumulation are demonstrated in Figure 2f, with similar results obtained in the SCC9 line (Supplementary Figure S1b online). Expression of a silencing-resistant PKP2 construct in PKP2 KD NHEKs reversed the phenotypes of increased zyxin accumulation (Figure 2g and h) and focal adhesion size (Figure 2i). Similar results were obtained in the SCC9 cell line (Supplementary Figure S1c-e online).

Wound healing is negatively affected by PKP2 silencing

We hypothesized that the PKP2 KD cells may exhibit impaired cell migration based on the increased presence of stress fibers and mature, enlarged focal adhesions, which are known impediments to cell motility (Desai *et al.,* 2004; Hamill *et al.,* 2009; Jackson *et al.,* 2011). To test this possibility, epithelial monolayers were subjected to a scratch wound and subsequently imaged over 16 hours and 30 minutes to follow wound closure (Figure 3a and b). Although control silenced cells closed wounds in ~10–12 hours, PKP2 KD monolayers displayed a transient lag in wound closure.

PKP2-null keratinocytes exhibit decreased focal adhesion turnover

The enlarged focal adhesions observed in PKP2 KD cells could be indicative of reduced focal adhesion turnover, resulting in the observed changes in migration described above. To address the possibility that focal adhesion turnover was affected by PKP2 loss, cells expressing green fluorescent protein (GFP)–vinculin or GFP–paxillin were imaged over time to analyze the fate of nascent focal adhesions (Figure 4). PKP2 KD cell adhesions were more stable with an average lifetime of 84 minutes, whereas the CTL KD cells exhibited focal adhesions with an average stability of only 37 minutes (Figure 4a and Supplementary Movies S1 and S2 online). Using fluorescence recovery after photobleaching (FRAP), we determined that the average half time of recovery of GFP– vinculin in PKP2 KD cells was 38.8 seconds (SEM±9.8), which was longer than the average half time of recovery for the

control cells at 26.4 seconds (SEM$\pm_{5.2}$, $P<0.05$; Figure 4b). Representative graphs from the FRAP analyses are shown in Figure 4c. These data demonstrate an impaired focal adhesion turnover upon loss of PKP2.

PKP2 regulates the levels of β1 and β4 integrins in keratinocytes

Interactions between the extracellular matrix and keratinocytes are mediated in large part by the engagement of the common keratinocyte integrins such as αv, α3, α6, β1, and β4, which can affect actin organization either directly or indirectly, as well as regulating cell attachment, migration, proliferation, and differentiation (Margadant *et al.,* 2010; Tsuruta *et al.,* 2011; Weber *et al.,* 2011). The aberrant migration and focal adhesion turnover of PKP2 KD cells could therefore be due to changes in integrin expression (Vega *et al.,* 2012). The expression of the β1 and β4 integrins was analyzed by immunofluorescence and immunoblot analyses, and an increased amount of both integrins was observed in PKP2 KD cells compared with the control keratinocytes (Figure 5a and b). Furthermore, an α and β integrin ELISA demonstrated that the surface expression of several α and β integrins was upregulated in PKP2 KD cells (Figure 5c). We considered the possibility that the increased integrin expression had a role in the focal adhesion pheno-types described above, as it has been reported that expression of α3β1 and α6β4 negatively regulates keratinocyte migration (Litjens *et al.,* 2006; Margadant *et al.,* 2009). To address this possibility, control and PKP2 KD cells were silenced for either β1 or β4 integrin. Silencing of β1 or β4 integrin did not affect the total levels of focal adhesion components such as talin, zyxin, and vinculin (Figure 6a and Supplementary Figure S2a online). However, the decreased expression of β1 integrin in the PKP2 KD cells (at least $5.7 \times$ less than the level expressed in the control cells) reversed the PKP2 KD phenotypes, with focal adhesion size and zyxin accumulation returning to the levels observed in control cells (Figure 6b, c, and d). Although this rescue could be due to changes directly linked to β1 signaling, it is also possible that a6b4 localization or function could be affected by β1 silencing (Margadant *et al.,* 2010). β4 silencing in the PKP2 KD cells (~$2.5 \times$ less than the level expressed in control cells) produced focal adhesions with a similar zyxin pixel intensity to the PKP2 KD cells, although the focal adhesions were smaller, more similar to the focal adhesions of the control cell population. The β4-silenced cells had a more marked substrate adhesion defect than the β1-silenced population. Interestingly, cells silenced for PKP2 and β1 expressed ~2 more β4 than the control cells, which may have compensated for the loss of β1 integrin to allow for substrate adhesion (Figure 6a and Supplementary Figure S2a online).

In an effort to uncover the potential mechanism by which PKP2 regulates protein expression of the integrins, we performed quantitative RT-PCR on control and PKP2-silenced cells to analyze the levels of β1 and β4 integrin in each population. Upon PKP2 silencing, there was an increase in both β1 and β4 mRNA expression by ~1.4-fold, demonstrating the possibility that PKP2 regulates the protein level of these integrins through mRNA (Figure 6e). It is not yet clear as to how PKP2 affects the levels of integrin mRNA in epithelial cells. PKP2 could affect mRNA transcription or stability, as another armadillo family member, plakoglobin, has recently been shown to affect fibronectin mRNA stability in keratinocytes (Todorovic *et al.,* 2010). In support of this possibility, PKP1 and PKP3 have been localized with RNA-binding proteins in cytoplasmic stress granules, and PKP2 has been discovered in nuclear

structures containing polymerase III (Mertens *et al.,* 2001; Hoffman *et al.,* 2006). A role for PKP2 in polymerase II structures, which are involved in integrin transcription, has not been reported (Hofmann *et al.,* 2006; Vigneault *et al.,* 2007). PKP2 could indirectly modulate integrin mRNA levels through focal adhesion components that contain LIM domains such as paxillin and zyxin that are known to shuttle to the nucleus and affect transcription (Wang and Gilmore, 2003; Hervy *et al.,* 2006). The integrins themselves can regulate gene expression through tension-induced recruitment of mRNA to adhesive zones (Chicurel *et al.,* 1998; Hervy *et al.,* 2006).

The focal adhesion phenotypes reported here could be due to the increased RhoA activity occurring as a result of PKP2 silencing (Godsel *et al.,* 2010). To address this possibility, we used Y27632, an inhibitor of the kinase ROCK (Rho-associated protein kinase), which is downstream of RhoA. Using low inhibitor amounts, the activity of the RhoA pathway in PKP2 KD cells was maintained similar to the CTL KD population, as indicated by myosin light chain phosphorylation (Figure 6f and Supplementary Figure S2b online). Although the activity of the RhoA pathway was decreased, the increased β1 and β4 observed in the PKP2 KD cells was not restored to control levels (Figure 6f). However, zyxin accumulation and focal adhesion size in PKP2 KD cells were brought to levels similar to that observed in the CTL KD cells (Figure 6g and h and Supplementary Figure S2c and d online). The finding that both integrin β1 silencing and RhoA activity modulation could restore the normal focal adhesion pheno-type suggests either a linear pathway regulated by PKP2 with integrins upstream of RhoA or, alternatively, PKP2 regulation of integrins and RhoA via two different routes, both having impacts on focal adhesions. The coordinated interaction between cell–cell junctions and cell–substrate attachments is necessary to form and maintain a stratified epidermis. Signaling scaffold proteins associated with either of these adhesive complexes may serve to integrate finely tuned signals within an adhesive network to regulate the morphogenesis, homeostasis, and wound healing of the skin. Spatiotemporal regulation of cell contacts in such an adhesive network is necessary for morphogenesis, for the homeostatic turnover of the epidermis, and for reepithelialization after wounding; therefore, misregulation of this process could contribute to inherited disease pathogenesis and cancer progression (Has and Bruckner-Tuderman, 2006; Muller *et al.,* 2008; Watt and Fujiwara, 2011; Epifano and Perez-Moreno, 2012). The data presented here support the hypothesis that the signaling scaffold PKP2, which is localized in the basal layer of the skin, modulates the formation of the cell–cell contact, the desmosome, and has a role in modulating cell–substrate adhesion.

MATERIALS AND METHODS

DNA constructs and siRNA

The siRNAs against human PKP2, β1 integrin, and β4 integrin, and nontargeting siRNAs were used for KD experiments (Thermo Fisher Scientific, Waltham, MA). The siRNA against human PKP2 (Smart Pool siGENOME, Thermo Fisher Scientific; 5′-GAGGAACCATTGCA GATTA-3′; 5′-CAACGTCACTGGATGCCTA-3′; 5′-GCACGCGACCT TCTAAACA-3′; 5′-GAGTATGTCTACAACCTAC-3′) has been well characterized. The silencing-resistant PKP2-FLAG construct has been described previously

(Bass-Zubek *et al.,* 2008; Godsel *et al.,* 2010). GFP-tagged vinculin and GFP-tagged paxillin were kind gifts from Dr Teng-Leong Chew (Northwestern University Feinberg School of Medicine, Chicago, IL).

Cell line electroporation and transfections and drug treatment

The SCC9 cell line (gift of L Hudson, University of New Mexico Albuquerque, NM; originally isolated by J Rheinwald, Harvard Medical School, Boston, MA) was maintained in DMEM/F-12 media, 10% fetal bovine serum, and 1% penicillin/streptomycin. Primary NHEKs were isolated from human foreskin as previously described (Halbert *et al.,* 1992). The cells were propagated in medium 154 supplemented with human keratinocyte growth supplement (Invitrogen, Grand Island, NY), and 0.07 m$_M$ CaCl$_2$. Transient transfections of complementary DNAs encoding for GFP-tagged proteins were performed on cultures grown on glass coverslips, or on 100- or 35-mm tissue culture dishes (Thermo Fisher Scientific, Pittsburgh, PA), using Exgen 500 reagent, according to the manufacturer's protocol (Fermentas Life Sciences, Glen Burnie, MD). GFP-tagged constructs and siRNAs were introduced into the normal human primary keratinocytes via electroporation (Amaxa Nucleofector, Lonza, Walkersville, MD). siRNAs were transfected into the SCC9 cell line using Dharmafect1 reagent (Thermo Fisher Scientific, Pittsburgh, PA) according to the manufacturer's protocol. siRNA was introduced at a concentration of 20 μ$_M$ (SCC9) or 50 μ$_M$ (NHEKs). The ROCK inhibitor Y27632 (Sigma, St Louis, MO) was used at a concentration of 1 μ$_M$–10 μ$_M$. Cells were incubated at 37 °C for several hours, and were lysed and subjected to SDS-PAGE and western blotting or cells were processed for immunofluorescence staining.

Antibodies

The following rabbit polyclonal antibodies were used: anti-zyxin (kind gift of Dr Mary Beckerle, University of Utah, Salt Lake City, UT), anti-p-paxillin (Cell Signaling, Beverly, MA), and anti-glyceraldehyde-3-phosphate dehydrogenase (anti-GAPDH; Sigma). The following mouse mAbs were used: clones PP2/62, PP2/86, PP2/150 anti-PKP2 supernatant (Progen Biotechnik, Heidelberg, Germany), anti-talin, Clone 8d4 (Sigma), anti-vinculin Clone hVIN1 (Sigma), anti-paxillin Clone 349 (BD Biosciences, San Jose, CA), anti-β1 integrin (3H1192; Santa Cruz Biotechnology, Santa Cruz, CA), and anti-b4 integrin Clone 7/CD104 (BD Biosciences). Photostable, Alexa Fluor-350–conjugated phalloidin was used to label actin, which is pseudocolored green in Figure 2e. Photostable, Alexa Fluor–conjugated secondary antibodies were used for indirect immunofluorescence analyses (Invitrogen, Carlsbad, CA): 488- or 568-conjugated goat anti-mouse or goat anti-rabbit IgG at 1:300 for immunofluorescence analyses (Invitrogen) and horseradish peroxidase–conjugated goat anti-mouse or goat anti-rabbit IgG at 1:5,000 for western blotting (Kirkegaard Perry Laboratories, Baltimore, MD).

Cell attachment and integrin-mediated cell adhesion assays

Collagen I and Collagen IV for attachment assays were purchased and used for thin-layer coating according to the manufacturer's protocols (BD Biosciences, San Jose, CA). Cells were fixed with paraformalde-hyde, stained using crystal violet, and counted using a spectrophotometer. For the α/β integrin–mediated cell adhesion assay, an ELISA assay was

performed according to the manufacturer's instructions (EMD Millipore, Billerica, MA). Briefly, cells were lifted from culture dishes using phosphate-buffered saline containing 5 m_M EDTA and 0.1% glucose and washed with the cell assay buffer provided in the kit. Cells were plated in triplicate in a concentration of 1×10^4 to 2×10^4 into wells containing anti-α or anti-β antibodies, or control wells, and incubated for 2 hours at 37 °C. Wells were washed and stained with the crystal violet stain solution for 5 minutes at room temperature, followed by dye extraction using the buffer provided in the kit, and the absorbance was read at 540 nm using a spectrophotometer.

Preparation of cell lysates for immunoblot analysis

Whole-cell lysates in Laemmli sample buffer were resolved by 7.5 or 14% SDS-PAGE and immunoblotted as previously described in Angst *et al.,* (1990). Immunoreactive proteins were visualized using enhanced chemiluminescence.

Focal adhesion turnover and FRAP analyses

For focal adhesion stability studies, cells expressing GFP-tagged vinculin or paxillin were imaged at 5-minute time points, and focal adhesions were followed from the time of formation to turnover. Control KD (33 cells) and PKP2 KD (25 cells) were imaged at 5-minute intervals and used for the calculations with 5–20 focal adhesions measured per cell. FRAP was analyzed by FRAPCalc program (Dr Rolf Sara, University of Turku, Turku, Finland). FRAP and live-cell imaging were performed on Andor CSUX1 Yokogawa (Belfast, Ireland) spinning disk confocal microscope fitted on a Nikon Ti PerfectFocus stand. Cell culture conditions were maintained by a TOKAI HIT stage-top CO_2-heated chamber (Shizuoka-Ken, Japan). Photoablation was performed using the galvo-controlled Andor FRAPPA unit, and image acquisition was performed on the Andor iXon EMCCD camera at 5-second intervals.

Immunofluorescence analysis and image acquisition

Cells were seeded onto glass coverslips for at least 48–72 hours after siRNA/ complementary DNA transfections or electroporations. Cover-slips were washed in phosphate-buffered saline and fixed for immunofluorescence in 4% paraformaldehyde at room temperature for 10 minutes. Primary/secondary antibody combinations are routinely tested to rule out nonspecific crossover. Primary antibody incubations were performed at 4 °C overnight in a humid chamber. Secondary antibody incubations were performed for 1 hour at 37 °C. In each case, control and treatment populations were manipulated identically throughout the experiment. Coverslips were mounted with polyvinyl alcohol (Sigma). Fixed cells were visualized with a Leica microscope (model DMR, Melville, NY), or a Leica DMI 6000B inverted microscope. The DMR microscope was fitted with 40 × (PL Fluotar, NA 1.0) and 63 × objectives (PL APO, NA 1.32), and images were captured with an Orca 100 CCD camera (model C4742-95; Hamamatsu, Bridgewater, NJ) and Metamorph 7.7 imaging software (Molecular Devices, Sunnyvale, CA). Images were cropped, brightened, and contrasted for optimal presentation using Adobe Photo-shop CS4 (Adobe, San Jose, CA), and the images were compiled into figures using Adobe Illustrator CS4 (Adobe).

Time-lapse imaging

Cells were seeded onto Lab-Tek chambered coverglass slides (Thermo Fisher Scientific, Pittsburgh, PA). For wound healing studies, the cell monolayers were grown to confluence and wounded with a 26-gauge needle. Normal primary human keratinocytes were imaged in growth medium (Medium 154 with supplements). SCC9 cells were incubated in imaging medium (Hanks' Balanced Salt Solution, 20 m$_M$ HEPES, 1% fetal bovine serum, 2 m$_M$ L-glutamine, 4.5 g l^{-1} glucose, and 1 m$_M$ amino acids; recipe courtesy of G Kreitzer, Weill Medical College of Cornell University, New York, NY). For cell spreading analyses, cells were incubated at 37 °C for 30–60 minutes before imaging. Time-lapse recordings were obtained at 5-minute intervals, as cells were imaged within a 37 °C environmental control system chamber using 100 W mercury halide fiber optic illumination. For fluorescence imaging, cells expressing GFP-tagged vinculin or paxillin were plated for 12–16 hours before imaging. Time-lapse images were captured with either a 10 × (HC FL Fluotar, NA 0.3), 20 × (HCX Fluotar, NA 0.4), 40 × (HCX Fluotar, NA 0.6), or 63 × objective (HCX PL APO, NA 1.4) using an ORCA-ER AG camera. Movies were compiled and images were further processed using ImageJ (http://rsb.info.nih.gov/ij/; National Institutes of Health) or the Metamorph 7.7 imaging software (Molecular Devices, Sunnyvale, CA).

Quantification of fluorescence intensity

Cell–substrate junctions were visualized in time-lapse images and from fixed populations of cells expressing GFP-tagged vinculin or paxillin (Dr Teng-Leong Chew, Northwestern University Feinberg School of Medicine). The fluorescence pixel intensity of cell–substrate contacts was determined by calculating the average pixel intensity within a region of interest made by tracing the cell–substrate contact from 12-bit images using the Metamorph 7.7 imaging software (Molecular Devices). Images are representative of three or more experiments. Intensities were plotted using whisker graphs to illustrate lower and upper extremes of fluorescence intensity and the lower and upper quartiles of the data sets, as well as median localization within the observed population. Slides were imaged within 3 days after processing, and all conditions in an experiment were imaged on the same day using the same instruments and exposure settings. For quantification analyses, >20 random areas per experimental group were imaged with the same exposure time and camera settings. Graphs were generated using Microsoft Office Excel 2007 (Microsoft, Redmond, WA).

Quantitative real-time reverse-transcriptase–PCR (qRT-PCR) analysis

RNA was isolated and purified from keratinocytes using Tri Reagent (Molecular Research Center, Cincinnati, OH) and the RNA Clean-up Kit (Qiagen, Valencia, CA) according to the manufacturer's recommendations. First-strand synthesis was performed on normalized RNA samples using SuperScript III First-Strand Synthesis SuperMix for qRTPCR Kit (Invitrogen). qRT-PCR was performed using SYBR Green PCR Master Mix (Life Technologies/Applied Biosystems, Grand Island, NY) with the following primers against human GAPDH, PKP2, ITGB1, and ITGB4: 5′-GACTTCTCCAACTCCATGTCC-3′ (human ITGB4, forward 1) and 5′-GTCCACAAACTTGCCAAATCC-3′ (hITGB4, reverse 1); 5^0-TGTAAGGAGAAGGATGTTGACG-3′ (hITGB1, forward 1) and 5′-CA ACCACACCAGCTACAATTG-3′ (hITGB1, reverse 12); 5′-TGATGGG

AGAAAAGCGATGAG-3′ (hPKP2, forward 1) and 5′-GCTGGTAG GAGAGGTTATGAAG-3′ (hPKP2, reverse 1); and 5′-ACATCGCTCA GACACCATG-3′ (hGAPDH, forward 1) and 5′-TGTAGTTGAG GTCAATGAAGGG-3′ (hGAPDH, reverse 1). Representative of at least four experiments performed in triplicate and normalized to GAPDH; error bars±SD.

Statistical analysis

Graphs were generated using Microsoft Office Excel 2007.

Error bars for fluorescence pixel intensity measurements represent SEMs or SD, as mentioned in each figure legend. Statistical analyses were performed using Student's two-tailed *t*-test.

Supplementary Material

Refer to Web version on PubMed Central for supplementary material.

Acknowledgments

Abbreviations

CTL	control
FRAP	fluorescence recovery after photobleaching
GFP	green fluorescent protein
KD	knockdown
NHEK	normal human epidermal keratinocyte
PKP	plakophilin
siRNA	small interfering RNA

REFERENCES

Angst BD, Nilles LA, Green KJ. Desmoplakin II expression is not restricted to stratified epithelia. J Cell Sci. 1990; 97:247–57. [PubMed: 2277092]

Bass-Zubek AE, Godsel LM, Delmar M, et al. Plakophilins: multi-functional scaffolds for adhesion and signaling. Curr Opin Cell Biol. 2009; 21:708–16. [PubMed: 19674883]

Bass-Zubek AE, Hobbs RP, Amargo EV, et al. Plakophilin 2: a critical scaffold for PKC alpha that regulates intercellular junction assembly. J Cell Biol. 2008; 181:605–13. [PubMed: 18474624]

Bolling MC, Jonkman MF. Skin and heart: une liaison dangereuse. Exp Dermatol. 2009; 18:658–68. [PubMed: 19558499]

Bonne S, Gilbert B, Hatzfeld M, et al. Defining desmosomal plakophilin-3 interactions. J Cell Biol. 2003; 161:403–16. [PubMed: 12707304]

Chen X, Bonne S, Hatzfeld M, et al. Protein binding and functional characterization of plakophilin 2. Evidence for its diverse roles in desmosomes and beta -catenin signaling. J Biol Chem. 2002; 277:10512–22. [PubMed: 11790773]

Chicurel ME, Singer RH, Meyer CJ, et al. Integrin binding and mechanical tension induce movement of mRNA and ribosomes to focal adhesions. Nature. 1998; 392:730–3. [PubMed: 9565036]

Choi CK, Zareno J, Digman MA, et al. Cross-correlated fluctuation analysis reveals phosphorylation-regulated paxillin-FAK complexes in nascent adhesions. Biophys J. 2011; 100:583–92. [PubMed: 21281572]

Desai LP, Aryal AM, Ceacareanu B, et al. RhoA and Rac1 are both required for efficient wound closure of airway epithelial cells. Am J Physiol Lung Cell Mol Physiol. 2004; 287:L1134–44. [PubMed: 15298851]

Epifano C, Perez-Moreno M. Crossroads of integrins and cadherins in epithelia and stroma remodeling. Cell Adh Migr. 2012; 6:261–73. [PubMed: 22568988]

Getsios S, Simpson CL, Kojima S, et al. Desmoglein 1-dependent suppression of EGFR signaling promotes epidermal differentiation and morphogenesis. J Cell Biol. 2009; 185:1243–58. [PubMed: 19546243]

Godsel LM, Dubash AD, Bass-Zubek AE, et al. Plakophilin 2 couples actomyosin remodeling to desmosomal plaque assembly via RhoA. Mol Biol Cell. 2010; 21:2844–59. [PubMed: 20554761]

Green KJ, Getsios S, Troyanovsky S, et al. Intercellular junction assembly, dynamics, and homeostasis. Cold Spring Harb Perspect Biol. 2010; 2:a000125. [PubMed: 20182611]

Green KJ, Simpson CL. Desmosomes: new perspectives on a classic. J Invest Dermatol. 2007; 127:2499–515. [PubMed: 17934502]

Halbert CL, Willam Demers G, Galloway DA. The E4 and E7 genes of human papillomavirus type 6 have weak immortalizing activity in human epithelial cells. J Virol. 1992; 66:2125–34. [PubMed: 1312623]

Hall A. Rho GTPases and the actin cytoskeleton. Science. 1998; 279:509–14. [PubMed: 9438836]

Hamill KJ, Hopkinson SB, DeBiase P, et al. BPAG1e maintains keratinocyte polarity through beta4 integrin-mediated modulation of Rac1 and cofilin activities. Mol Biol Cell. 2009; 20:2954–62. [PubMed: 19403692]

Hamill KJ, Hopkinson SB, Hoover P, et al. Fibronectin expression determines skin cell motile behavior. J Invest Dermatol. 2012; 132:448–57. [PubMed: 21956124]

Hamill KJ, Hopkinson SB, Jonkman MF, et al. Type XVII collagen regulates lamellipod stability, cell motility, and signaling to Rac1 by targeting bullous pemphigoid antigen 1e to alpha6beta4 integrin. J Biol Chem. 2011; 286:26768–80. [PubMed: 21642434]

Hamill KJ, Paller AS, Jones JC. Adhesion and migration, the diverse functions of the laminin alpha3 subunit. Dermatol Clin. 2010; 28:79–87. [PubMed: 19945619]

Has C, Bruckner-Tuderman L. Molecular and diagnostic aspects of genetic skin fragility. J Dermatol Sci. 2006; 44:129–44. [PubMed: 16996720]

Hatzfeld M. Plakophilins: Multifunctional proteins or just regulators of desmosomal adhesion? Biochim Biophys Acta. 2007; 1773:69–77. [PubMed: 16765467]

Hatzfeld M, Haffner C, Schulze K, et al. The function of plakophilin 1 in desmosome assembly and actin filament organization. J Cell Biol. 2000; 149:209–22. [PubMed: 10747098]

Hervy M, Hoffman L, Beckerle MC. From the membrane to the nucleus and back again: bifunctional focal adhesion proteins. Curr Opin Cell Biol. 2006; 18:524–32. [PubMed: 16908128]

Hoffman LM, Jensen CC, Kloeker S, et al. Genetic ablation of zyxin causes Mena/VASP mislocalization, increased motility, and deficits in actin remodeling. J Cell Biol. 2006; 172:771–82. [PubMed: 16505170]

Hofmann I, Casella M, Schnolzer M, et al. Identification of the junctional plaque protein plakophilin 3 in cytoplasmic particles containing RNA-binding proteins and the recruitment of plakophilins 1 and 3 to stress granules. Mol Biol Cell. 2006; 17:1388–98. [PubMed: 16407409]

Hong IK, Jeoung DI, Ha KS, et al. Tetraspanin CD151 stimulates adhesion-dependent activation of Ras, Rac, and Cdc42 by facilitating molecular association between beta1 integrins and small GTPases. J Biol Chem. 2012; 287:32027–39. [PubMed: 22843693]

Jackson B, Peyrollier K, Pedersen E, et al. RhoA is dispensable for skin development, but crucial for contraction and directed migration of keratinocytes. Mol Biol Cell. 2011; 22:593–605. [PubMed: 21209320]

Litjens SH, de Pereda JM, Sonnenberg A. Current insights into the formation and breakdown of hemidesmosomes. Trends Cell Biol. 2006; 16:376–83. [PubMed: 16757171]

Margadant C, Charafeddine RA, Sonnenberg A. Unique and redundant functions of integrins in the epidermis. FASEB J. 2010; 24:4133–52. [PubMed: 20624931]

Margadant C, Raymond K, Kreft M, et al. Integrin alpha3beta1 inhibits directional migration and wound re-epithelialization in the skin. J Cell Sci. 2009; 122:278–88. [PubMed: 19118220]

McGrath JA, Mellerio JE. Ectodermal dysplasia-skin fragility syndrome. Dermatol Clin. 2010; 28:125–9. [PubMed: 19945625]

Mertens C, Hofmann I, Wang Z, et al. Nuclear particles containing RNA polymerase III complexes associated with the junctional plaque protein plakophilin 2. Proc Natl Acad Sci USA. 2001; 98:7795–800. [PubMed: 11416169]

Muller EJ, Williamson L, Kolly C, et al. Outside-in signaling through integrins and cadherins: a central mechanism to control epidermal growth and differentiation? J Invest Dermatol. 2008; 128:501–16. [PubMed: 18268536]

Ren XD, Kiosses WB, Dieg DJ, et al. Focal adhesion kinase suppresses Rho activity to promote focal adhesion turnover. J Cell Sci. 2000; 113:3673–8. [PubMed: 11017882]

Rickelt S, Pieperhoff S. Mutations with pathogenic potential in proteins located in or at the composite junctions of the intercalated disk connecting mammalian cardiomyocytes: a reference thesaurus for arrhythmogenic cardiomyopathies and for Naxos and Carvajal diseases. Cell Tissue Res. 2012; 348:325–33. [PubMed: 22450909]

Schober M, Raghavan S, Nikolova M, et al. Focal adhesion kinase modulates tension signaling to control actin and focal adhesion dynamics. J Cell Biol. 2007; 176:667–80. [PubMed: 17325207]

Sklyarova T, Bonné S, D'Hooge P, et al. Plakophilin-3 -deficient mice develop hair coat abnormalities and are prone to cutaneous inflammation. J Invest Dermatol. 2008; 128:1375–85. [PubMed: 18079750]

Sobolik-Delmaire T, Reddy R, Pashai A, et al. Plakophilin-1 localizes to the nucleus and interacts with single-stranded DNA. J Invest Dermatol. 2010; 130:2638–46. [PubMed: 20613778]

Thomason HA, Scothern A, McHarg S, et al. Desmosomes: adhesive strength and signalling in health and disease. Biochem J. 2010; 429:419–33. [PubMed: 20626351]

Todorovic V, Desai BV, Patterson MJ, et al. Plakoglobin regulates cell motility through Rho- and fibronectin-dependent Src signaling. J Cell Sci. 2010; 123:3576–86. [PubMed: 20876660]

Tsuruta D, Hashimoto T, Hamill KJ, et al. Hemidesmosomes and focal contact proteins: functions and cross-talk in keratinocytes, bullous diseases and wound healing. J Dermatol Sci. 2011; 62:1–7. [PubMed: 21376539]

Vega FM, Colomba A, Reymond N, et al. RhoB regulates cell migration through altered focal adhesion dynamics. Open Biol. 2012; 2:120076. [PubMed: 22724071]

Vigneault F, Zaniolo K, Gaudreault M, et al. Control of integrin genes expression in the eye. Prog Retin Eye Res. 2007; 26:99–161. [PubMed: 17194617]

Wang Y, Gilmore TD. Zyxin and paxillin proteins: focal adhesion plaque LIM domain proteins go nuclear. Biochim Biophys Acta. 2003; 1593:115–20. [PubMed: 12581855]

Watt, FM.; Fujiwara, H. Cell-extracellular matrix interactions in normal and diseased skin. Vol. 3. Cold Spring Harb Perspect Biol; 2011. p. a005124

Weber GF, Bjerke MA, DeSimone DW. Integrins and cadherins join forces to form adhesive networks. J Cell Sci. 2011; 124:1183–93. [PubMed: 21444749]

Wolf A, Krause-Gruszczynska M, Birkenmeier O, et al. Plakophilin 1 stimulates translation by promoting eIF4A1 activity. J Cell BIol. 2010; 188:463–71. [PubMed: 20156963]

Yoshigi M, Hoffman LM, Jensen CC, et al. Mechanical force mobilizes zyxin from focal adhesions to actin filaments and regulates cytoskeletal reinforcement. J Cell Biol. 2005; 171:209–15. [PubMed: 16247023]

Zhang J, Betson M, Erasmus J, et al. Actin at cell-cell junctions is composed of two dynamic and functional populations. J Cell Sci. 2005; 118:5549–62. [PubMed: 16291727]
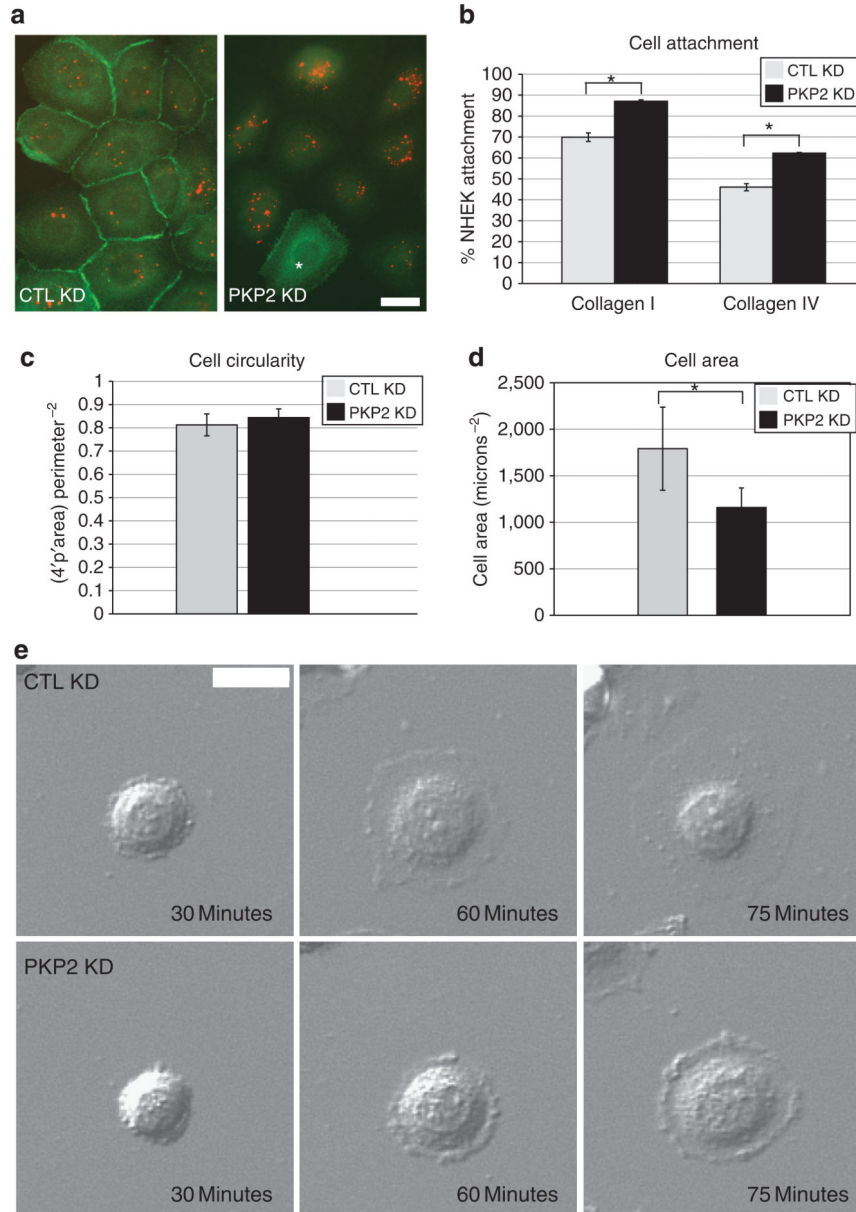
Figure 1. Plakophilin 2 (PKP2) affects cell attachment and spreading

(**a**) PKP2 expression was analyzed in control (CTL knockdown (KD)) or PKP2-silenced normal human epidermal keratinocytes (NHEKs; PKP2 KD) and correlated with the presence of siGLO, a small interfering RNA (siRNA) uptake efficiency marker. Whereas 89% of the NHEKs were silenced for PKP2, correlating with siGLO, 4% of the PKP2-silenced cells did not exhibit siGLO fluorescence. Of those cells that still retained PKP2 expression, only 5% contained siGLO. The cell indicated with the asterisk has escaped PKP2 silencing (green), correlating with the absence of siGLO (red). (**b**) A total of 85% and >60% of the PKP2 KD NHEKs bound to collagen I and IV, respectively, whereas 70% and 45% of CTL KD cells bound to the substrate. (**c**) NHEK cell circularity was calculated during 90 minutes of attachment. (**d**) PKP2-silenced NHEKs exhibited ~30% smaller cell

areas than controls. (**e**) Representative images demonstrate spreading efficiency in control NHEKs compared with PKP2 KD cells (*$P<0.05$, error bars $\pm_{SEM,}$ scale bar ¼ 20 µm).
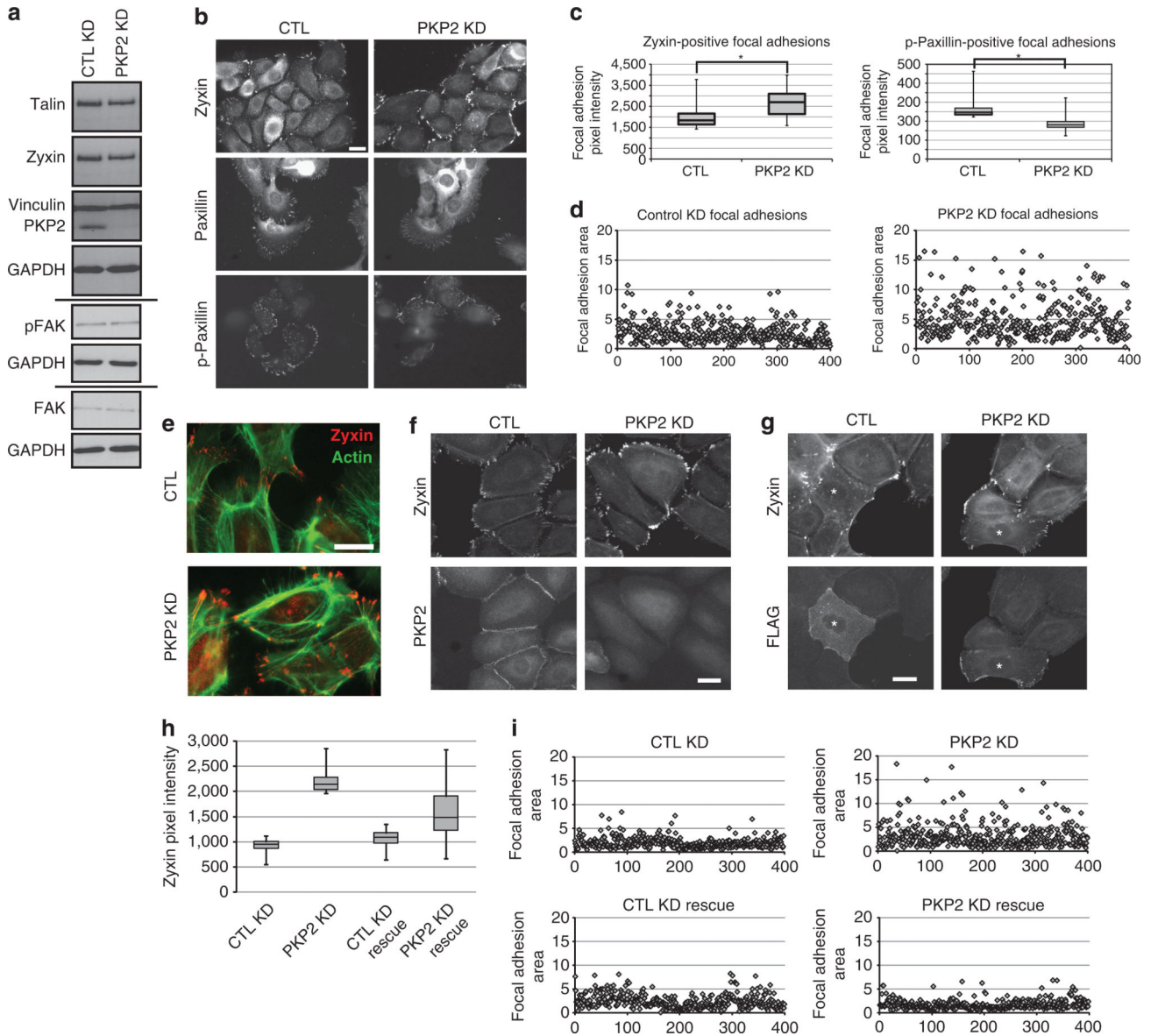
Figure 2. Plakophilin 2 (PKP2)-silenced cells exhibit large, mature focal adhesions
(**a**) Immunoblot analysis of control (CTL) and PKP2 knockdown (KD) normal human epidermal keratinocytes (NHEKs) demonstrated no change in focal adhesion components. FAK, focal adhesion kinase; GAPDH, glyceraldehyde-3-phosphate dehydrogenase. (**b**) Zyxin, paxillin, and phospho-paxillin (p-Paxillin) localized to NHEK focal adhesions. (**c**) Whisker graphs of the pixel intensities of focal adhesion maturity indicators, zyxin and phospho-paxillin (*$P<0.05$). The increased zyxin and a decreased phospho-paxillin in PKP2 KD focal adhesions suggests a more mature phenotype. (**d**) Scatter plots in which each diamond represents the area of a zyxin-stained focal adhesion. PKP2 KD cells exhibit focal adhesions ~2 × larger than controls. (e–h) Expression of a silencing-resistant PKP2.FLAG construct in PKP2 KD NHEK cells brings zyxin accumulation and focal adhesion size to normal levels. Scale bar = 20 μm.
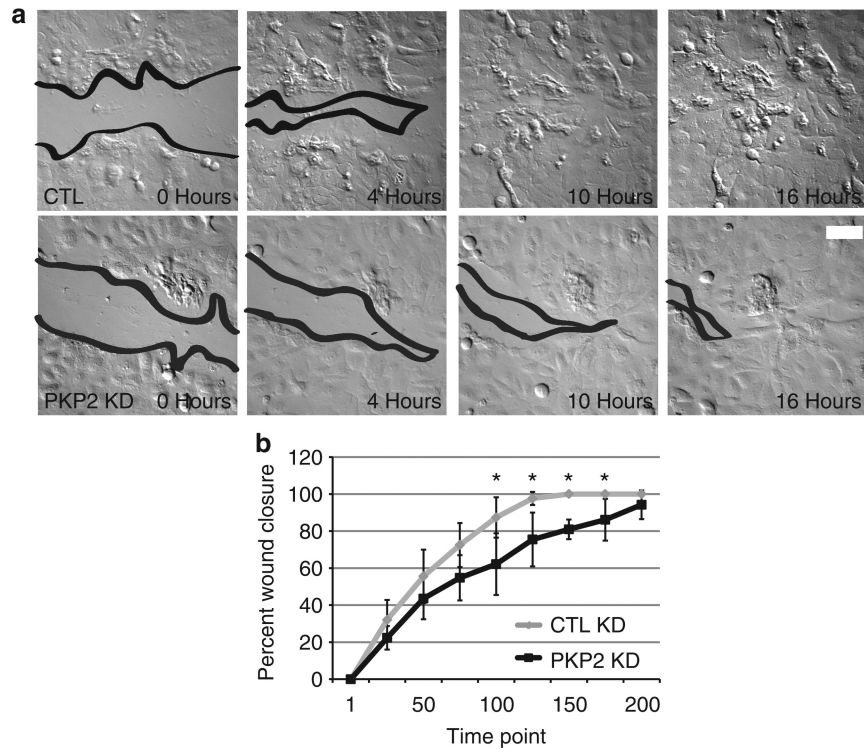
Figure 3. Cell migration is impaired upon plakophilin 2 (PKP2) silencing
(**a, b**) PKP2 knockdown (KD) SCC9 cells closed wounds more slowly than the control (CTL) cells that closed wounds at 10–11 hours of imaging (*$P<0.05$, error bars $\pm_{SEM}$, scale bar = 80 μm).
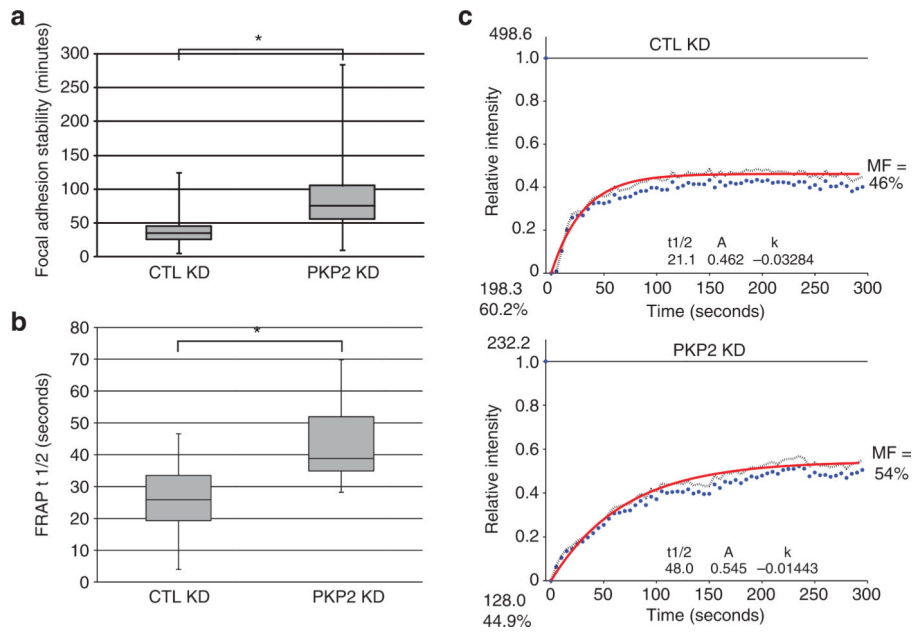
Figure 4. Focal adhesion turnover is decreased upon plakophilin 2 (PKP2) knockdown (KD)
(**a**) Keratinocytes expressing green fluorescent protein (GFP)–tagged paxillin were imaged at 5-minute intervals, and the stability of nascent focal adhesions was measured over time. Representative movies of normal human epidermal keratinocytes (NHEKs) used for these measurements presented in the whisker graphs are included as Supplementary Movies S1 and S2 online. *P<0.5. (**b**) The recovery rate for GFP–vinculin was longer in the PKP2 KD focal adhesions of SCC9 and NHEKs with an average half time of recovery of 38.8 seconds compared with the control population at 26.4 seconds. *P<0.5. (**c**) Typical fluorescence recovery after photobleaching (FRAP) curves of GFP–vinculin in control (CTL KD) and PKP2-silenced SCC9 cells (PKP2 KD). MF, mobile fraction.
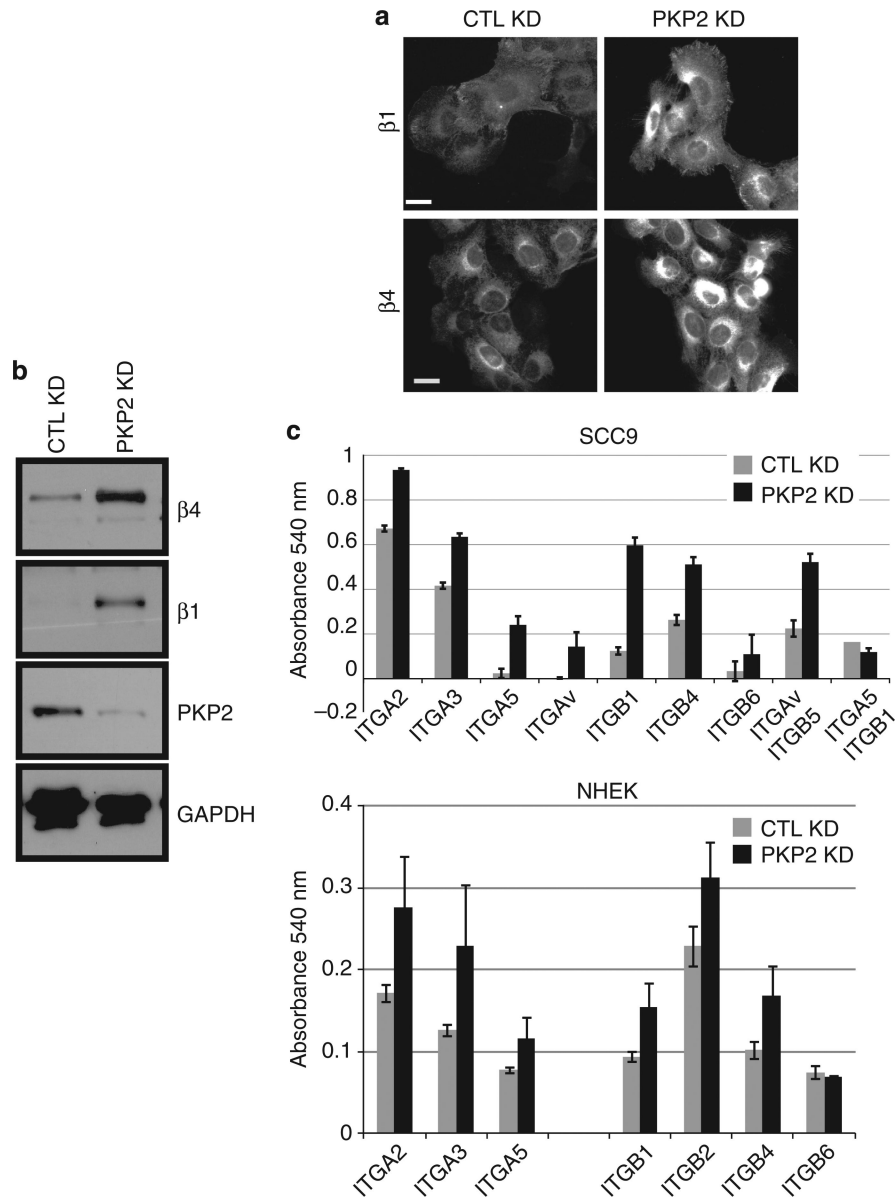
Figure 5. The expression of β1 and β4 integrin is increased upon plakophilin 2 (PKP2) silencing
(**a**) Staining of control (CTL) and PKP2-silenced normal human epidermal keratinocytes (NHEKs) demonstrates an increased amount of β1 and β4 integrin expressed by the PKP2 knockdown (KD) cells. Scale bar = 20 μm. (**b**) Whole-cell lysates of NHEKs demonstrate an elevated amount of both β1 and β4 integrin in steady-state PKP2 KD keratinocyte cultures compared with control cells. GAPDH, glyceraldehyde-3-phosphate dehydrogenase. (**c**) An α and β integrin ELISA demonstrates an increased amount of α and β integrin subunits expressed on the surface of SCC9 cells or NHEKs silenced for PKP2 (error bars ±SEM).
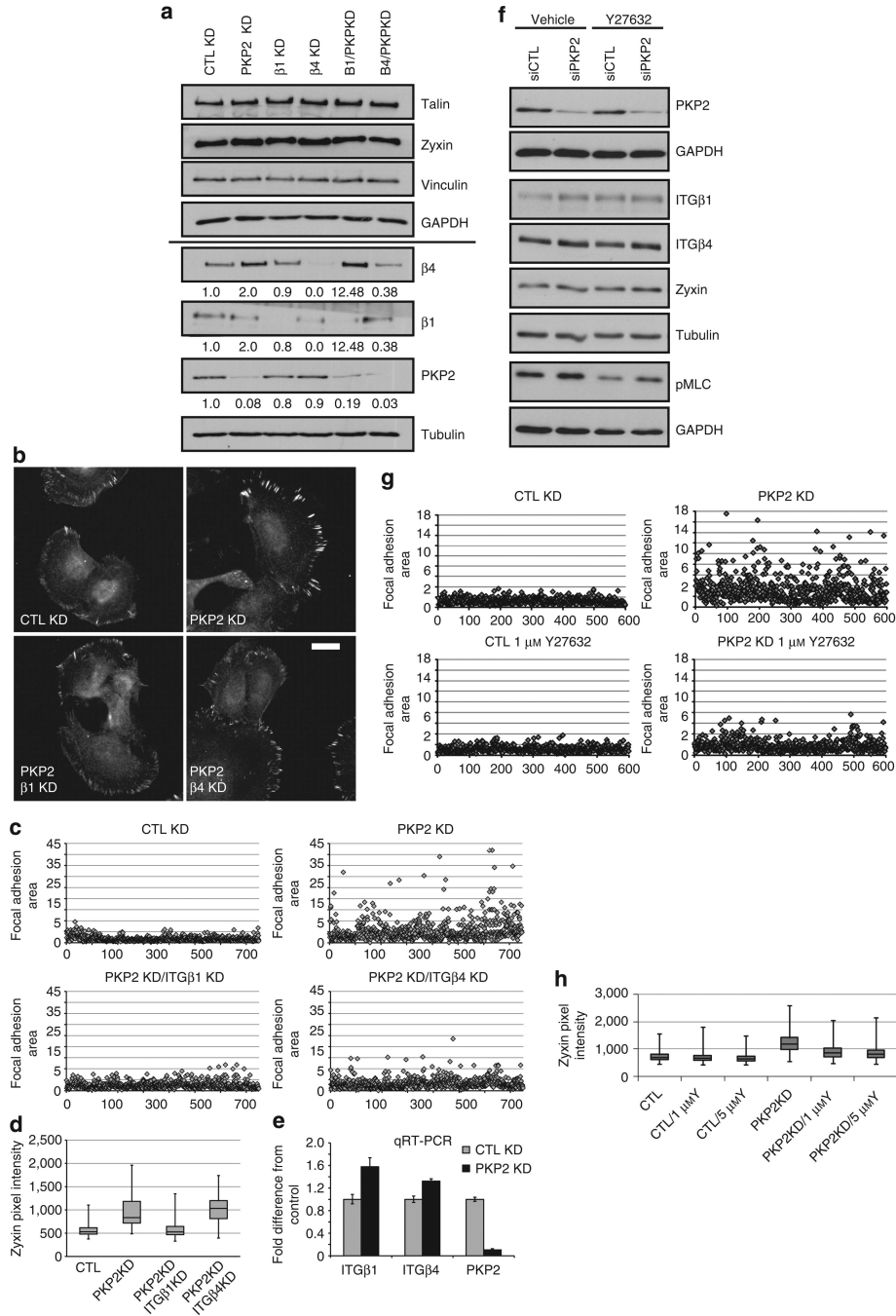
Figure 6. The silencing of β1 rescues the focal adhesion turnover phenotype of plakophilin 2 (PKP2) knockdown (KD) cells

(**a**) Control (CTL) or PKP2 KD cells were silenced for β1 or β4 integrin, and the expression of β1, β4, talin, zyxin, and vinculin was analyzed, with no change to focal adhesion components observed. GAPDH, glyceraldehyde-3-phosphate dehydrogenase. (**b**) Immunofluorescence analysis, (**c**) focal adhesion size, and (**d**) zyxin accumulation (scale bar = 20 μm). PKP2 KD normal human epidermal keratinocytes (NHEKs) silenced for β1 integrin displayed a recovery of focal adhesion size and zyxin pixel intensities. The

silencing of β4 integrin silencing decreased focal adhesion size, but did not rescue zyxin accumulation. (**e**) Quantitative RT-PCR (qRT-PCR) analysis demonstrates increased β1 and β4 mRNA levels in PKP2 KD cells (error±SD). (**f**) The expression of β1, β4, zyxin, and phosphorylated myosin light chain (pMLC) after treatment with the ROCK (Rho-associated protein kinase) inhibitor Y27632. RhoA signaling activity is decreased (indicator, pMLC) without rescuing the increased β1 and β4 expression in PKP2 KD cells. (**g, h**) Y27632 treatment of PKP2 KD cells brings focal adhesion size and zyxin accumulation to normal levels.